Improved sliding mode control for wind turbine under wind speed variation

Abdelhaq.Amar bensaber[1] **Abdelmadjid.Guerouad**[1] **Abdelkader Belhachemi**[1] **Mohammed Amar bensaber**[2]
abs.abdelhak@gmail.com a.guerouad@yahoo.com hachemiaek@ymail.com m.amarbensaber@esi-sba.dz

[1]AVCIS Laboratory - Oran University of Science and Technology - Mohamed Boudiaf –
[2]School of Computer Science 08 May 1945 Sidi Bel Abbès

Abstract— *Doubly Fed Induction Generator is very popular in variable speed wind power plants[1, 2] because of it advantages like lessen losses , minimum cost ,an improved efficiency and active and reactive power control capabilities[2]. Traditionally their control is based on PI a controller which is advisable for linear time invariant systems. However, the components in wind turbines work as nonlinear systems where electromechanical parameters change frequently [3]. This paper proposes a first order sliding mode control however such control may excite unmodeled high frequency system transients due to chattering phenomenon. The aim of the proposed controller is to contribute with some important features such as chatter free performance and heftiness in terms of transient response of the nonlinear systems subjected to dynamic conditions such as lower and higher wind speeds, robustness and secure power system operation. The wind turbine is validated in the Matlab/Simulink environment and the simulation results obtained confirm the performance of the proposed control*

Keywords-component; *SMC,Doubly fed induction generator (DFIG).Active and Reactive Power control, Maximum power point tracking, MPPT,Sliding mode control.*

I. Introduction

Nowadays, energy production is moving towards the renewable energy sources because of the desire to reduce dependence on fossil fuels and the global warming issues. Wind energy is consider a good technology advances for it reliability and cost efficiency [4, 5]. Therefore, those factors become important topics in industry and research [6, 7]. Therefore, control strategies are needed to achieve maximum performance, which means seeking the maximum power from the wind energy source using MPPT. The doubly fed induction generator based wind turbine has been an attractive choice [8, 9] due to the independent active and reactive control and it ability to provide variable speed due to control of back-to-back converter scheme[10, 11], other advantages of the DFIG WTs is reducing mechanical stresses, compensate for torque and power pulsations[12] and improve power quality[2] ,the main advantage of the DFIG is that the rotor side converter is only sized for 30% of rated power which mean the cost of the converter is reduced[13], still the reaction of DFIG to grid voltage disturbances is sensitive, as described in [14] for symmetrical and unsymmetrical voltage dips it is necessary to protect for the rotor side converter. To be able to stay connected to the grid even with faults it is required to control wind powers [2, 14-16], these control schemes are based on the vector control concept with classical control techniques such as the PI controllers, but this controllers can only provide good performance under ideal grid voltage conditions. Furthermore, disturbances and parameter variations will provide insufficient performance. Therefore, papers have presented different control schemes for DFIG such as Sliding Mode Control, high order sliding mode control [6, 15-18], smart control or adaptive algorithms [1, 19, 20]. Nonlinear control methodologies gained attraction such as Sliding Mode Control have recently. Although very robust and accurate, standard SMC suffers from two major drawbacks. First, the chattering phenomena resulting from the high frequency control switching which severely restricts its application to wind power systems since it deteriorates the control performance and excites high frequency oscillations [21, 22]. In order To deal with these difficulties, several modifications to the original sliding control law have been proposed, the most popular being the boundary layer approach [15, 23, 24].

In this present paper, a regulation in the power exchanged between the machine and the grid based on the Sliding Mode Controller (SMC) is proposed and to overcome it drawbacks we decide to use a simple method instead of complicate the system with higher order control, this method is obtained by adjusting the discontinuous control signal across the sliding surface, PI and SMC controllers are compared and results are discussed, the objective is to show that controllers as (SMC) can improve performances of doubly-fed induction generators in terms of reference tracking, sensibility to perturbations and parameters variations. This paper is organized as follows; firstly, turbine model and the Maximum Power Tracking are presented in section II. In section III, the mathematical model of DFIG is introduced. Section IV presents Active and Reactive Power .In section V the sliding

mode controller is proposed. In section VII, matlab simulation results are shown and discussed.

II. MODEL OF THE TURBINE:

The power contained in the form of kinetic energy at a speed V_v, surfaceA_1, is expressed by

$$P_v = \frac{1}{2}\rho A_1 V_v^3 \quad (1)$$

Where ρ is the air density, but the wind turbine is can regain only a part of that power:

$$P_v = \frac{1}{2}\rho \pi R^2 V_v^3 C_p \quad (2)$$

Where: R is the radius of the wind turbine; Cp is the power coefficient, a dimensionless parameter that expresses the effectiveness of the wind turbine in the transformation of kinetic energy of the wind into mechanical energy[23]. For a given wind turbine, this coefficient is a function of wind speed, the speed of rotation of the wind turbine, and the pitch angle. Cp is often given as a function of the tip speed ratio λ, defined by:

$$\lambda = \frac{R\Omega_t}{V_v} \quad (3)$$

Where R is the length of the blades (radius of the turbine rotor), Ω_t is the angular speed of the rotor. The theoretical maximum value of C_p is given by the Betz limit:

$$C_{p\_theo\_\max} = 0,593 = 59,3\%$$

The torque and power coefficient C_p is represented in function of tip step ratio (λ) and the pitch angle (β) as fellow:

$$C_p = C_1\left(\frac{C_2}{\lambda_i} - C_3\beta - C_4\beta^{C_5} - C_6\right)\left(e^{C_7/\lambda_i}\right) \quad (4)$$

$$\lambda_i = \frac{1}{\lambda + C_8} \quad (5)$$

The mechanical torque C_t on the slow shaft of the turbine can be expressed by:

$$C_t = \frac{P_t}{\Omega_t} = \frac{\pi}{2\lambda}\rho R^3 v^2 C_p \quad (6)$$

A. Mechanical System: The mechanical model will be illustrated in Figure 1

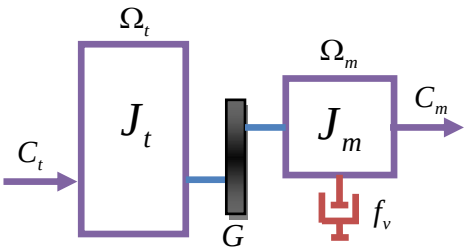

Figure 1 : Mechanical model

Where: J_t: the turbine side masses, while J_m : the electrical machine mass, G is the gearbox ratio. The turbine speed and the fast shaft torque are expressed in by:

$$\Omega_m = G\Omega_t \quad (7) \qquad C_m = C_t / G \quad (8)$$

Next,
$$C_m - C_{em} = \left(\frac{J_t}{G^2} + J_m\right)\frac{d\Omega_m}{dt} + f_v\Omega_m \quad (9)$$

B. Maximum Power Tracking MPPT

Following the path of maximum power extraction is the main objective of the speed control. Many methods are proposed to ensure the following of the maximum power extraction trajectory [25, 26]. In this paper we will use the direct speed controller (DSC) shown in fig 2, it concept is based on generating the optimal turbine rotational speed for each wind speed value, and use it speed reference. Then, with the help of a regulator the turbine rotational speed is controlled. For a given operating point (speed of fixed wind), it is desired that the mechanical power is maximum, the reference rotational speed of the turbine is obtained from the equation is defined by:

$$\Omega_t^* = \left(\lambda_{opt} v\right)/R \quad (10) \quad \text{Thus,} \quad \Omega_m^* = G\Omega_t^* \quad (11)$$

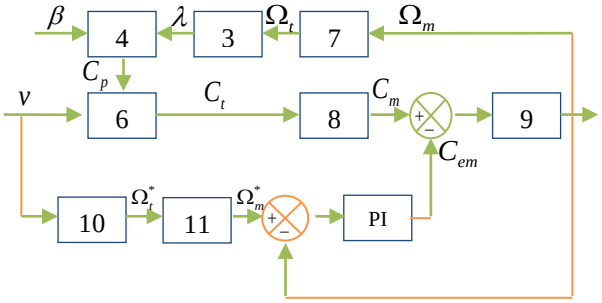

Figure 2 :Direct speed control.

We obtain the active power reference by the following equation:

$$P_{s\_ref} = C_{cem\_ref}\Omega_m \quad (12)$$

III. MATHEMATICAL MODEL OF DFIG:

We have chosen to use the double-fed induction generator because with the help of the bidirectional converter in the rotor it is possible to work in both sub-synchronous and super-synchronous. The electrical model of the machine obtained using Park transformation is given by the following equations [23, 26, 27]:

Stator, rotor voltages: Eqts (13-16)

$$V_{qs} = R_s I_{qs} + \frac{d\phi_{qs}}{dt} - \omega_s\phi_{ds} \; ; \; V_{ds} = R_s I_{ds} + \frac{d\phi_{ds}}{dt} - \omega_s\phi_{qs}$$

$$V_{dr} = R_r I_{dr} + \frac{d\phi_{dr}}{dt} - \omega\phi_{qr} \; ; \; V_{qr} = R_r I_{qr} + \frac{d\phi_{qr}}{dt} - \omega\phi_{dr}$$

Where: $\omega = \omega_s - \omega_m \quad (17)$

Stator, rotor fluxes:

$$\phi_{ds} = L_s I_{ds} + M I_{dr} \quad (18) \qquad \phi_{qs} = L_s I_{qs} + M I_{qr} \quad (19)$$

$$\phi_{dr} = L_r I_{dr} + M I_{ds} \quad (20) \qquad \phi_{qr} = L_r I_{qr} + M I_{qs} \quad (21)$$

The electromagnetic torque is:

$$C_{em} = P\left(\phi_{ds} I_{qs} - \phi_{qr} I_{ds}\right) = PM\left(I_{dr} I_{qs} - I_{qr} I_{ds}\right) \quad (22)$$

The motion equation is:

$$C_{em} - C_r = J\frac{d}{dt}\Omega_m + f_v \Omega_m \quad (23) \quad J = \frac{J_{turbine}}{G^2} + J_g \quad (24)$$

Where: the load torque is C_r, J is the total inertia, mechanical speed is Ω_r.

IV. The DFIG Vector Control:

In this section, the application of vector control DFIG is to achieve a decoupling between the quantities generating torque and flux. For this, we adjust the flux by (I_{ds} or I_{dr}), and torque by (I_{qs} or I_{qr}). Thus, the dynamics of DFIG will be reduced to that of a DC machine. This method can be outlined as shown in Fig 3.

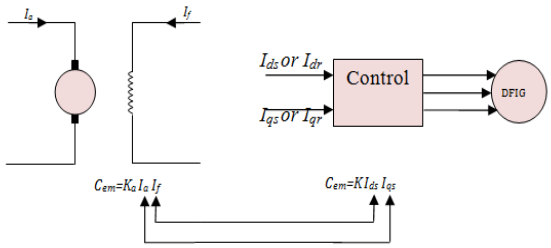

Figure 3 : Analogy between the vector control of DFIG and the control of a DC machine.

The doubly fed induction generator model can be described by the next equations in the synchronous frame whose axis d is aligned with the stator flux vector as shown in fig. 4, ($\phi_{ds} = \phi_{qs}$) and ($\phi_{qs} = 0$) [7, 23, 26, 28]. By neglect stator resistances voltage will be:

$$V_{ds} = 0 \quad \text{and} \quad V_{qs} = V_s = \omega_s \phi_s \quad (25)$$

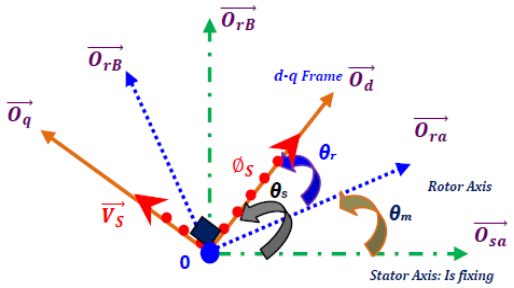

Figure 4 : Stator and rotor flux vectors in the synchronous d-q Frame.

We driver to an uncoupled power control; where, I_{dr} controls the active power, and the reactive power is controlled by the direct component I_{ds} [29]as shown in fig. 5:

$$P_s = -V_s \frac{M}{L_s} I_{qr} \quad (26)$$

$$Q_s = \left(\frac{\phi_s V_s}{L_s} - \frac{M}{L_s} V_s I_{dr}\right) = \left(\frac{V_s^2}{\omega_s L_s} - \frac{M}{L_s} V_s I_{dr}\right) \quad (27)$$

The equations of the voltages according to the rotor currents are shown below (fig. 5):

$$V_{dr} = R_r I_{dr} + L_r \sigma \frac{dI_{dr}}{dt} - L_r \sigma \omega I_{qr} \quad (28)$$

$$V_{qr} = R_r I_{qr} + L_r \sigma \frac{dI_{qr}}{dt} - L_r \sigma \omega I_{dr} + \frac{M}{L_s}\omega \phi_s \quad (29)$$

With: $$\sigma = \left(1 - M^2\right) / L_s L_r \quad (30)$$

Where: V_{dr}, V_{qr} are rotor voltage components; R_r is the rotor resistances; L_r, L_s are the rotor inductances; M is mutual inductance; σ is leakage factor; ω is the rotor pulsation .

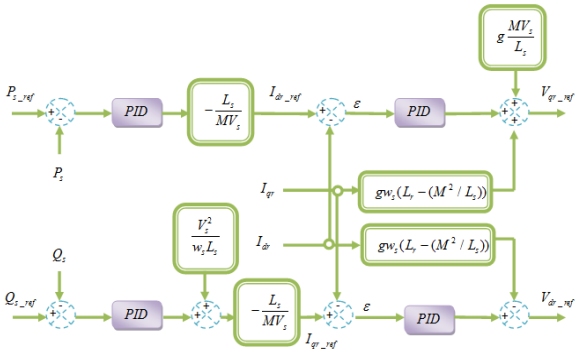

Figure 5 : The Conventional Active and Reactive Power Control of a DFIG.

V. The sliding mode control

The main advantage of this control is its simplicity and robustness in spite of uncertainties in the system and external disturbances and on the other hand it needs relatively less information about the system and also is insensitive to the parametrical changes of the system plus it doesn't need to the mathematical models accurately like classical controllers but needs to know the range of parameter changes for ensuring sustainability and condition satisfactory [15-18]. The sliding mode control has three stages: Choice of surface, Convergence condition and Calculation of the control laws.

Active and reactive power control:

$n = 1$, the power control equation will be defined by:

$$\begin{cases} S(P) = e_p = P_{ref} - P \\ S(Q) = e_Q = Q_{ref} - Q \end{cases} \quad (31)$$

Active power:

$$\dot{S}(P) = \dot{e}_P = \dot{P}_{s\_ref} - \dot{P}_s = \dot{P}_{s\_ref} + V_s \frac{M}{L_s} \dot{I}_{qr} \quad (32)$$

Substituting the expression of the power by the expression given in (16), the equation will become:

$$\dot{e}_P = \dot{P}_{s\_ref} + V_s \frac{M}{L_s L_r \sigma}\left(V_{qr} - R_r I_{qr} + g w_s L_r \sigma I_{dr} + g \frac{M V_s}{L_s} \right) \quad (33)$$

We replace V_{qr} with $V_{qreq} + V_{qrn}$,

$$\dot{e}_P = \dot{P}_{s\_ref} + V_s \frac{M}{L_s L_r \sigma}\left(\left(V_{qreq} + V_{qrn} \right) - R_r I_{qr} + g w_s L_r \sigma I_{dr} + g \frac{M V_s}{L_s} \right) \quad (34)$$

V_{qreq} and V_{qrn} are used to constraint the system to converge to $S_{dq} = 0$ The control vector V_{qrn} is obtained by imposing $\dot{S}_{dq} = 0$ and $V_{qrn} = 0$,so the equivalent control components are given by the following relation:

$$0 = \dot{P}_{s\_ref} + V_s \frac{M}{L_s L_r \sigma}\left(V_{qreq} - R_r I_{qr} + g w_s L_r \sigma I_{dr} + g \frac{M V_s}{L_s} \right) \quad (35)$$

Thus, $$V_{qreq} = -\frac{L_s L_r \sigma}{M V_s} \dot{P}_{s\_ref} + R_r I_{qr} - g w_s L_r \sigma I_{dr} - g \frac{M V_s}{L_s} \quad (36)$$

$$V_{qrn} = K_{Vqr} sign\left(S(P) \right) \quad (37)$$

Where, K_{Vqr} Is positive constant

Reactive power:

The same thing goes for the reactive power

$$\dot{S}(Q) = \dot{e}_Q = \dot{Q}_{s\_ref} - \dot{Q}_s = \dot{Q}_{s\_ref} + V_s \frac{M}{L_s} \dot{I}_{dr} \quad (38)$$

Substituting the expression of the power by the expression given in (15), the equation will become:

$$\dot{e}_Q = \dot{Q}_{s\_ref} + V_s \frac{M}{L_s L_r \sigma}\left(V_{dr} - R_r I_{dr} + g w_s L_r \sigma I_{qr} \right) \quad (39)$$

We replace V_{dr} with $V_{dreq} + V_{drn}$,

$$\dot{e}_Q = \dot{Q}_{s\_ref} + V_s \frac{M}{L_s L_r \sigma}\left(\left(V_{dreq} + V_{drn} \right) - R_r I_{dr} + g w_s L_r \sigma I_{qr} \right) \quad (40)$$

V_{qreq} and V_{qrn} will be the two components of the control vector used to constraint the system to converge to $S_{dq} = 0$ .The control vector V_{qrn} is obtain by imposing $\dot{S}_{dq} = 0$ and $V_{qrn} = 0$,so the equivalent control components are given by the following relation :

$$0 = \dot{Q}_{s\_ref} + V_s \frac{M}{L_s L_r \sigma}\left(V_{dreq} - R_r I_{dr} + g w_s L_r \sigma I_{qr} \right) \quad (41)$$

$$V_{dreq} = -\frac{L_s L_r \sigma}{M V_s} \dot{Q}_{s\_ref} + R_r I_{dr} - g w_s L_r \sigma I_{qr} \quad (42)$$

$$V_{drn} = K_{Vdr} sign\left(Q(P) \right) \quad (43)$$

Where, K_{Vdr} Is positive constant

The function sign is defined as:

$$sign(\phi) = \begin{cases} 1 \ , if \quad \phi \succ 0 \\ 0 \ , if \quad \phi = 0 \\ 1 \ , if \quad \phi \prec 0 \end{cases}$$

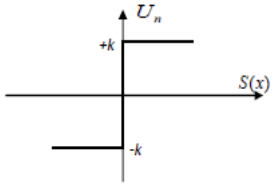

Figure 6 : Sign Function.

However, the latter generates on the sliding surface, a phenomenon called chattering, which is generally undesirable because it adds to the spectrum control high frequency components.

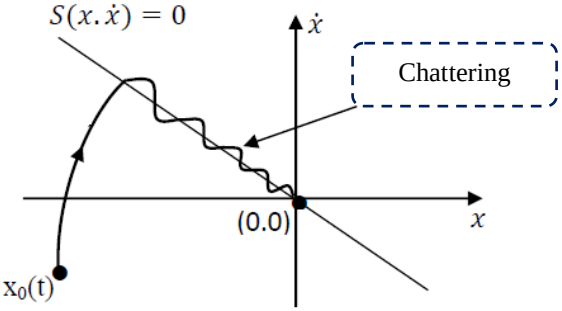

Figure 7: Chattering Phenomenon.

Solution proposed

In Order to minimize the chattering we will change the sign function with hyperbolic tangent function which will smooth the control signal across the sliding surface, the function is shown in Figure 6 and it's defined by:

$$U_n = K \frac{S(x)}{|S(x)| + \delta} + \eta \quad (44)$$

Thus,

$$\delta = \begin{cases} \delta_0 & \text{if } |S(x)| \geq \varepsilon \\ \delta_0 + \gamma \int S(x) dt & \text{if } |S(x)| \prec \varepsilon \end{cases} \quad (45)$$

$$\eta = \begin{cases} 0 & \text{if } |S(x)| \geq \varepsilon \\ \xi \int S(x) dt & \text{if } |S(x)| \prec \varepsilon \end{cases} \quad (46)$$

Where: $\delta, \eta, \xi, \varepsilon, \gamma$ are positive constants.

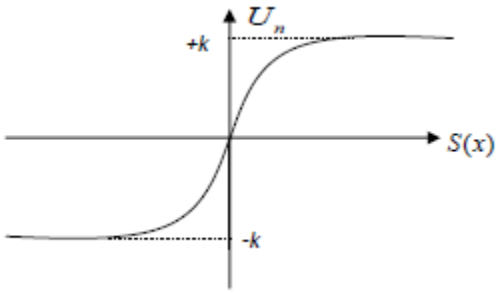

Figure 8 : hyperbolic tangent function.

VI. SIMULATION RESULTS

In this section, simulation tests have been performed using Matlab –Simulink environment. A comparison of the performances of the DFIG with two different linear and nonlinear controllers “PI, SMC and TAN-SMC” will be introduced and discussed

Reference tracking

The first test a change in wind speed is applied as shown in Fig (9) and in order to evaluate the MPPT control strategy proposed.

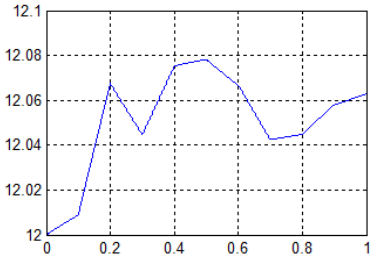

Figure 9 : Wind speed

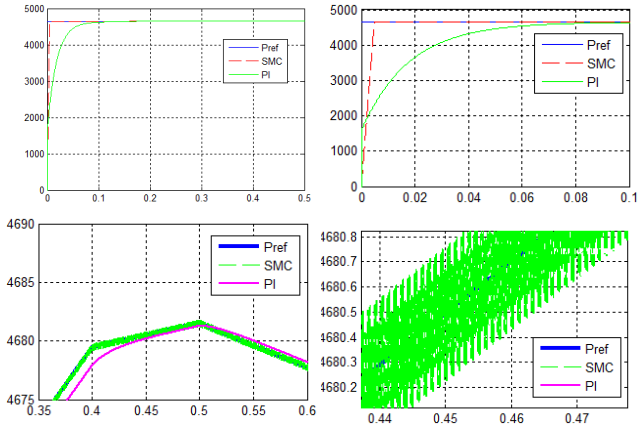

Figure 10 : Stator Active power Ps

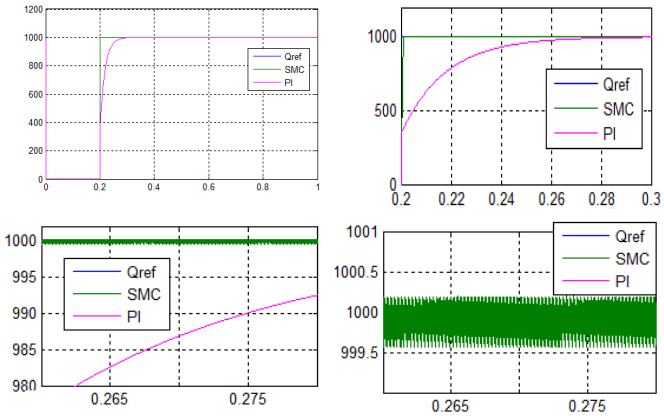

Figure 11 : Reactive Active power Qs

Hyperbolic Tangent Function:

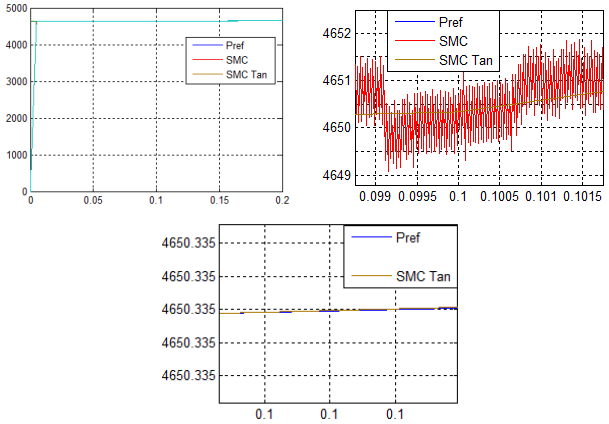

Figure 12 : Stator Active power Ps

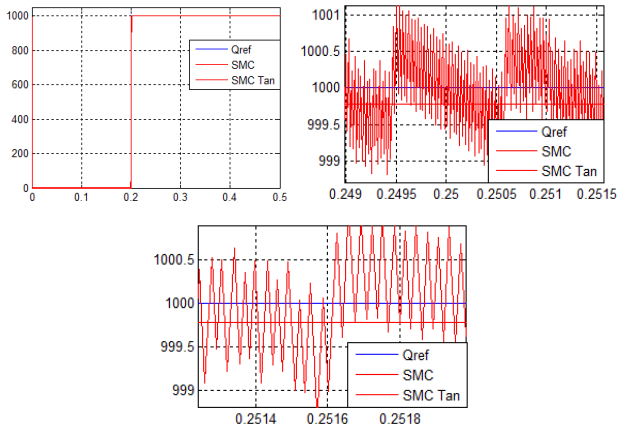

Figure 13 : Reactive Active power Qs

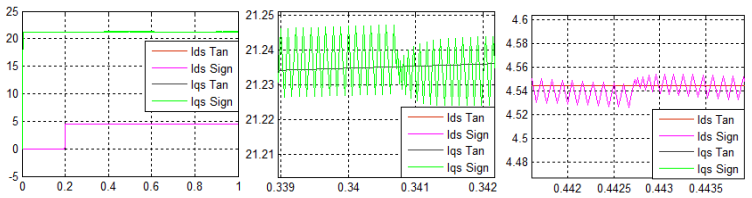

Figure 14 : stator current components

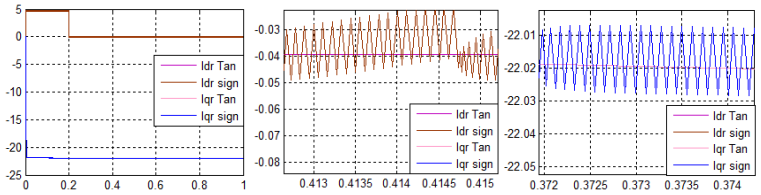

Figure 15 : Rotor current components

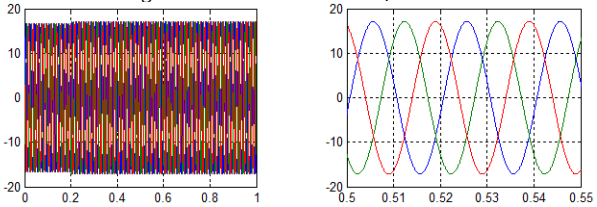

Figure 16 : stator current

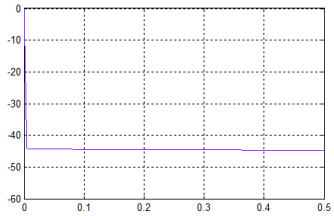

Figure 17 : Electromagnatique couple

The electromagnetic torque is shown in Fig (17) is negative due to the generator operation. We can notice a very good decoupling between the two components of the rotor and stator current is obtained as shown in fig 14-15 ensuring a decoupled control of powers Fig 8 and 9 represent the stator active and reactive powers and its reference profiles using PI regulator and Sliding mode control, we can notice that the dynamic response of the stator active power and reactive power under SMC control is much faster than that under the conventional PI control and it tracks almost perfectly their references .However, the SMC controller includes the presence of perturbations in its synthesis and we can notice that through the chattering phenomenon after zooming we can see clearly that the hyperbolic tangent function could smooth control signals and that caused an elimination of chattering phenomenon. This result is interesting for wind energy applications to ensure stability and quality of the generated power when the speed is varying.

VII. CONCLUSION

The PI controller although it's very popular, simple and mostly used in the industry it's not suitable for linear time invariant systems. In this paper, a wind turbine with a doubly fed induction generator is presented with the consideration of turbine variable velocity state and design controller for DFIG in form of using the sliding mode control then a solution to improve the control was proposed, simulation results show that the proposed controller provides a notable efficiency, since it permits to track the optimum power quickly despite the speed wind changing. On the other hand, the stator power quantities provided show smooth waveforms, with good tracking indices. Consequently, undesirable mechanical stresses and the chattering phenomena in the case of SMC are avoided

APPENDIX

The machine's parameters are presented below:
Stator resistance: Rs = 1.2Ω, Rotor resistance: Rr = 1.8Ω
Stator inductance: Ls = 0.1554H, Rotor inductance: Lr= 1.558 H, Mutual inductance: M = 0.15, Rated voltage: Vs=380 V/220V; Number of pole pairs: P= 2, Friction coefficient: Fr=0.0027N.s/rad, Frequency: f=50Hz; The moment of inertia: J=0.042 kg.m2, Aerodynamic coefficients C1=0.5, C2=116, C3=0.4, C4=0, C5=5, C6=21, controller parameter:

$$K_p = \frac{t_r}{L_r},\ K_i = \frac{K_p R_r}{L_r \sigma},\ K_{p\_Ir} = \frac{L_s L_r \sigma}{M V_s t_r},$$

$$K_{i\_Ir} = \frac{K_{p\_Ir} R_r}{L_r \sigma}$$

References

[1] A.M. Kassem, K.M. Hasaneen, A.M. Yousef, Dynamic modeling and robust power control of DFIG driven by wind turbine at infinite grid, International Journal of Electrical Power & Energy Systems 44(1) (2013) 375-382.
[2] N.H. Saad, A.A. Sattar, A.E.-A.M. Mansour, Low voltage ride through of doubly-fed induction generator connected to the grid using sliding mode control strategy, Renewable Energy 80 (2015) 583-594.
[3] D.H. Phan, S. Huang, Super-Twisting Sliding Mode Control Design for Cascaded Control System of PMSG Wind Turbine, Journal of Power Electronics 15(5) (2015) 1358-1366.
[4] H.T. Jadhav, R. Roy, A comprehensive review on the grid integration of doubly fed induction generator, International Journal of Electrical Power & Energy Systems 49 (2013) 8-18.
[5] S. Abdeddaim, A. Betka, Optimal tracking and robust power control of the DFIG wind turbine, International Journal of Electrical Power & Energy Systems 49 (2013) 234-242.
[6] E.C. López, J. Persson, High-Order Models of Doubly Fed Induction Generators, Wind Power in Power Systems, John Wiley & Sons, Ltd2012, pp. 849-864.
[7] M. Yamamoto, O. Motoyoshi, Active and reactive power control of doubly-fed wound rotor induction generator, 21st Annual IEEE Conference on Power Electronics Specialists, 1990, pp. 455-460.
[8] H. Li, Z. Chen, Overview of different wind generator systems and their comparisons, IET Renewable Power Generation, Institution of Engineering and Technology, 2008, pp. 123-138.
[9] A. Hansen, P. Sø rensen, F. Blaabjerg, F. Iov, {Centralised power control of wind farm with doubly fed induction generators}, Renewable Energy 31(7) (2006) 935-951.
[10] N.D. Caliao, Dynamic modelling and control of fully rated converter wind turbines, Renewable Energy 36(8) (2011) 2287-2297.
[11] F.E.V. Taveiros, L.S. Barros, F.B. Costa, Back-to-back converter state-feedback control of DFIG (doubly-fed induction generator)-based wind turbines, Energy 89 (2015) 896-906.
[12] W. Qiao, Dynamic modeling and control of doubly fed induction generators driven by wind turbines, 2009 IEEE/PES Power Systems Conference and Exposition, 2009, pp. 1-8.
[13] T. Ahmed, K. Nishida, M. Nakaoka, A Novel Stand-Alone Induction Generator System for AC and DC Power Applications, IEEE Transactions on Industry Applications 43(6) (2007) 1465-1474.
[14] J. Lopez, P. Sanchis, X. Roboam, L. Marroyo, Dynamic Behavior of the Doubly Fed Induction Generator During Three-Phase Voltage Dips, IEEE Transactions on Energy Conversion 22(3) (2007) 709-717.
[15] J.B. Alaya, A. Khedher, M.F. Mimouni, Nonlinear vector control strategy applied to a variable speed DFIG generation system, Eighth International Multi-Conference on Systems, Signals & Devices, 2011, pp. 1-8.
[16] Y. Shtessel, C. Edwards, L. Fridman, A. Levant, Sliding Mode Control and Observation, Springer New York2013.
[17] J.J.E. Slotine, W. Li, Applied Nonlinear Control, Prentice-Hall1991.
[18] B. Yang, L. Jiang, L. Wang, W. Yao, Q.H. Wu, Nonlinear maximum power point tracking control and modal analysis of DFIG based wind turbine, International Journal of Electrical Power & Energy Systems 74 (2016) 429-436.
[19] Z. Song, T. Shi, C. Xia, W. Chen, A novel adaptive control scheme for dynamic performance improvement of DFIG-Based wind turbines, Energy 38(1) (2012) 104-117.
[20] D. Zhi, L. Xu, J.A. Morrow, Improved direct power control of doubly-fed induction generator based wind energy generation system, 2007, pp. 436-441.
[21] M.J. Morshed, A. Fekih, A new fault ride-through control for DFIG-based wind energy systems, Electric Power Systems Research 146 (2017) 258-269.
[22] J.G. Njiri, D. Söffker, State-of-the-art in wind turbine control: Trends and challenges, Renewable and Sustainable Energy Reviews 60 (2016) 377-393.

[23] G. Abad, J. López, M.A. Rodríguez, L. Marroyo, G. Iwanski, Direct Control of the Doubly Fed Induction Machine, Doubly Fed Induction Machine, John Wiley & Sons, Inc.2011, pp. 363-477.
[24] A. Luna, F.K.A. Lima, P. Rodriguez, E.H. Watanabe, R. Teodorescu, Comparison of power control strategies for DFIG wind turbines, 2008 34th Annual Conference of IEEE Industrial Electronics, 2008, pp. 2131-2136.
[25] S.E. Aimani, Modélisation des différentes technologies d'éoliennes intégrées dans un réseau de moyenne tension, 2004.
[26] F. Poitiers, ETUDE ET COMMANDE DE GENERATRICES ASYNCHRONES POUR L'UTILISATION DE L'ENERGIE EOLIENNE
 - Machine asynchrone à cage autonome
 - Machine asynchrone à double alimentation reliée au réseau, Université de Nantes, 2003.
[27] X. Lie, P. Cartwright, Direct active and reactive power control of DFIG for wind energy generation, IEEE Transactions on Energy Conversion 21(3) (2006) 750-758.
[28] M. Rahimi, M. Parniani, Dynamic behavior analysis of doubly-fed induction generator wind turbines – The influence of rotor and speed controller parameters, International Journal of Electrical Power & Energy Systems 32(5) (2010) 464-477.
[29] K. Jemmli, M. Jemli, M. Gossa, M. Boussak, Power flow control and VAR compensation in a doubly fed induction generator, International Journal of Sciences and Techniques of Automatic control & computer engineering, Special issue CEM (2008) 548-565.